

DENSITY DEPENDENCE OF SOLAR EMISSION LINES OF BORON-LIKE IONS*

B. N. DWIVEDI

Applied Physics Section, Institute of Technology, Banaras Hindu University, Varanasi-221005, India

and

P. K. RAJU

Indian Institute of Astrophysics, Bangalore-560034, India

(Received 11 December, 1979; in revised form 17 March, 1980)

Abstract. Steady state level density of 20 levels of boron-like ions, Mg VIII and Si X, have been computed as a function of electron density and temperature. We have accounted for collisional and spontaneous radiative processes. Photo-excitation between the two levels of the ground term has also been considered. Using the computed level density, line intensities have been obtained as a function of electron density and temperature. In case of Mg VIII, line intensity ratio $I(430.47)/I(436.62)$ is found to be electron density sensitive. Likewise other pairs of lines namely, $I(75.03)/I(74.86)$, $I(315.02)/I(430.47)$, and $I(315.02)/I(335.23)$ are also found to be density sensitive. Similar density sensitive line intensity ratios have been found for Si X. Absolute line fluxes from these ions at earth distance have been computed and are found to be comparable with values obtained, using various satellite and rocket measurements.

1. Introduction

One of the problems of EUV solar spectroscopy is to find electron density and temperature diagnostics for the solar chromosphere-corona transition region. With the advent of rocket, satellite and skylab probes there is currently considerable interest in finding electron density and temperature diagnostics for application to the solar atmosphere. Some of our efforts in this direction have already appeared in the literature (Elwert and Raju, 1975; Raju, 1978; Raju and Dwivedi, 1978, 1979).

The lines in the beryllium-like ions have been widely used as a density diagnostic (Munro *et al.*, 1971; Jordan, 1971; Gabriel and Jordan, 1972; Louergue and Nussbaumer, 1976; and Dufton *et al.*, 1978). Lines emitted from boron-like ions have also received considerable attention to probe the solar atmosphere (Elwert and Raju, 1975; Flower and Nussbaumer, 1975a, b). However, detailed investigation of lines emitted from Mg VIII ion as a potential candidate for density diagnostic has not been reported in the literature till recently. In the process of completion of this work, we learnt that Vernazza and Mason (1978) have also noted similar density sensitivity in case of EUV lines from Mg VIII ion. In the present investigation we have considered the first 20-levels of boron-like ions which include some X-ray lines also. Integrated line fluxes using a working model by Elzner (1976) have also been computed. The ${}^2P_{3/2}^{\circ} - {}^2P_{1/2}^{\circ}$ transition gives lines with wavelengths 3.03μ for

* Paper presented at the 5th Astronomical Society of India Meeting, held at Uttar Pradesh State Observatory, Naini Tal, India, 5-9 November, 1979.

Mg VIII and 1.43μ for Si X which have been observed (Munch *et al.*, 1967; Olsen *et al.*, 1971). Therefore, the present study of line emission from boron-like ions is a detailed one and covers X, EUV, and infra-red region. According to the ionization equilibrium calculations of Jordan (1969), Mg VIII has maximum relative ion abundance at 8×10^5 K and Si X at 1.6×10^6 K. Because of its maximum relative ion abundance around 8×10^5 K, lines emitted from Mg VIII are most suitable to probe chromosphere-corona transition region and possibly coronal hole regions of the solar atmosphere. Though a detailed computation on Si X has been reported (Elwert and Raju, 1975), we have included Si X in our study in the light of more accurate atomic data available at present. Furthermore, some more physical processes neglected by Elwert and Raju (1975) in their computation have been included in the present investigation. These additional ones are mentioned later in Section 3 (Dwivedi, 1979).

2. Energy Level Diagram for Boron-Like Ions

The schematic energy level scheme comprising the first 20 levels of boron-like ions is shown in Figure 1. The ground configuration $2s^2 2p$ is split into two levels $^2P_{1/2}^\circ$ and $^2P_{3/2}^\circ$ whereas the higher configuration includes $2s 2p^2$, $2p^3$, $2s^2 3s$, $2s^2 3p$, and $2s^2 3d$ states. The collisional processes have been shown by continuous lines and the radiative processes by broken lines.

To set up the necessary steady state equilibrium equations for various levels, the following physical processes have been considered:

(1) The doublet levels of the ground term have been linked through electron as well as proton collisional excitations and de-excitations; radiative excitation and spontaneous radiative decay.

(2) The quartet 4P term, in the configuration $2s 2p^2$ is connected to the ground term by collisional excitations, collisional de-excitations and radiative de-excitations. Collisional excitations and de-excitations between the levels of quartet 4P term have also been considered.

(3) The higher doublet terms are collisionally excited from the two levels of the ground term and decay by spontaneous radiative transitions. In addition, some levels may also be populated by cascade from still higher levels as indicated in Figure 1.

(4) The quartet $^4S^\circ$ term, in the configuration $2p^3$, is populated by collisional excitations from the lower quartet 4P term as well as from the doublet ground term and depopulated by spontaneous radiative transitions to the lower quartet 4P term.

The radiative excitation rates for the permitted transitions have been neglected since the lines corresponding to these transitions are in the X- and EUV regions of the spectrum and are optically thin. Moreover, at the temperatures of interest, recombinations for the levels considered have also been neglected compared to the electron excitations.

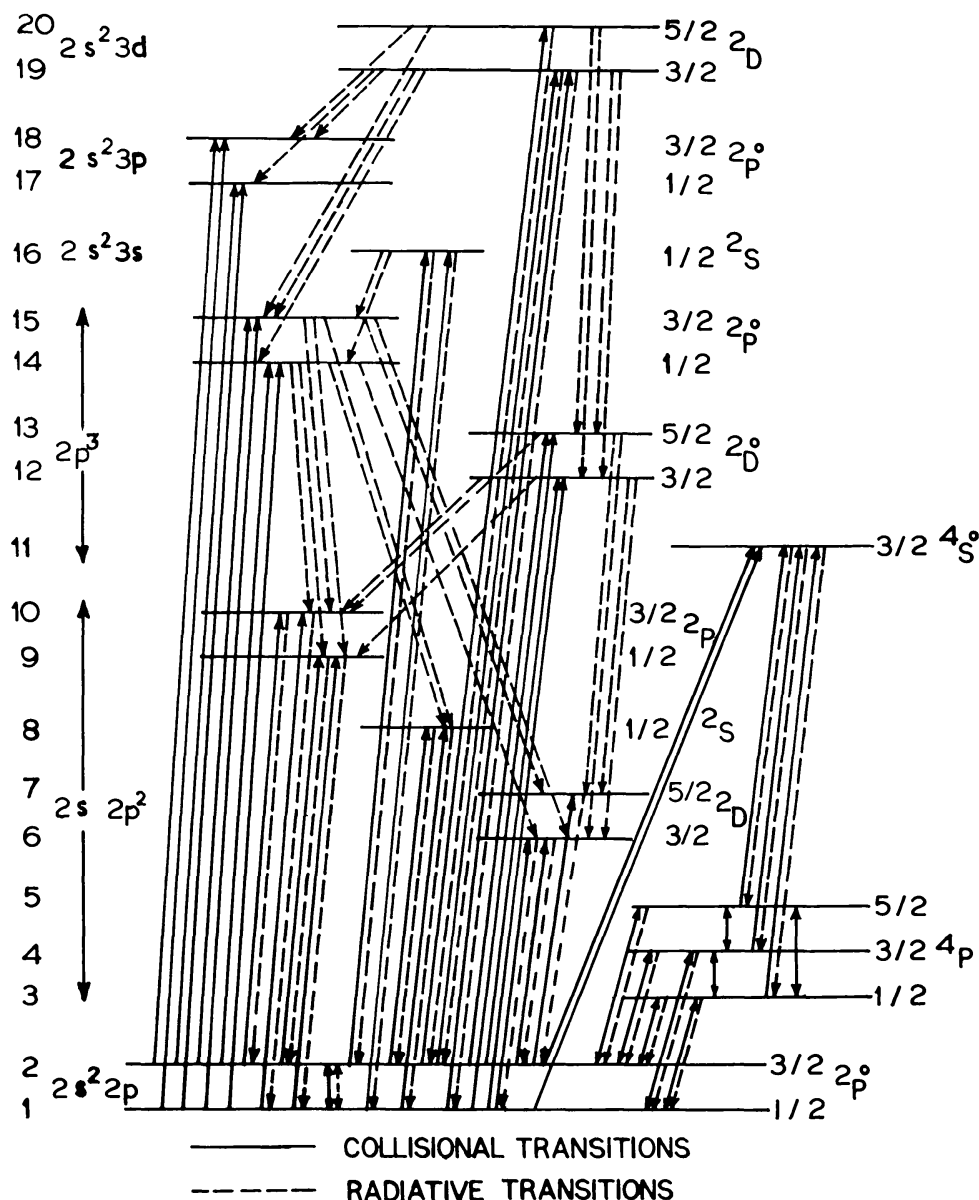


Fig. 1. Energy level scheme for boron-like ions: — collisional transitions, - - - radiative transitions.

3. Atomic Data

The appropriate atomic data required in the present study have been taken from the reported results in the literature. Wherever the relevant atomic data are not available, the existing data have been interpolated or extrapolated to obtain the working values. The atomic data (collision strengths and transition probabilities) for most of the important transitions have been taken from the recent computations of Dankwort and Trefftz (1976, 1977, 1978). The atomic data used by Elwert and Raju (1975) are mostly scaled values. Further, they have not taken into account proton excitation and de-excitation between the ground term levels; electron collisional excitations and de-excitations between the quartet 4P term in their computation.

Collision strengths for excitation between the quartet 4P term, have been taken from Flower and Nussbaumer (1975b). Proton excitation rate between the ground term levels have been taken from Bely and Faucher (1970). Some of the transition probability values have been taken from Wiese *et al.* (1969) and Shamey (1971). Wavelengths for the various transitions have been taken from Kelly and Palumbo (1973), Wiese *et al.* (1969), and Shamey (1971).

The photo-excitation rate R_{ij} between the $^2P^o$ ground term levels is important. The photo-excitation rate in the present study has been obtained using the expression (De Boer *et al.*, 1972)

$$R_{ij} = \frac{\omega_j}{\omega_i} A_{ji} (e^{h\nu_{ij}/kT_r} - 1)^{-1} D, \quad (1)$$

where D is the dilution factor, ω the statistical weight, A_{ji} spontaneous transition probability, ν_{ij} the frequency of the transition, and T_r is the radiation temperature. The dilution factor has been assumed to be equal to 0.5 in all cases for the sake of simplicity in computation. Using the continuum flux at a given wavelength (Labs and Neckel, 1968; Allen, 1973), we have computed the mean T_r from solar black body emission formula given by

$$J_\nu = \frac{2h\nu^3}{C^2} (e^{h\nu/kT_r} - 1)^{-1}. \quad (2)$$

The value of T_r obtained from Equation (2) is substituted in Equation (1) to obtain the corresponding values of R_{ij} . The radiation temperature obtained for Mg VIII at wavelength 3.03μ is $T_r = 6043$ K and for Si x at wavelength 1.43μ is $T_r = 6098$ K.

4. Level Population

The line emission from a given volume element in the solar atmosphere in a steady state is given by the expression

$$E(j, i) = \frac{1}{4\pi} A_{ji} h\nu_{ij} N_j \text{ (ergs cm}^{-3} \text{ s}^{-1} \text{ sr}^{-1}\text{)}, \quad (3)$$

where N_j is the level density for the upper level of the transition. Thus the problem reduces to the calculation of the population density (N_j) of the upper excited level. In order to evaluate N_j , statistical equilibrium equations have been set up by taking into account all the physical processes mentioned in Section 2. The level populations as a function of electron density and temperature have been evaluated by solving all the detailed balance equations for the atomic levels shown in Figure 1. Equilibrium equation for a given level (j) is in general expressed as

$$\begin{aligned} N_j \left[\sum_{i < j} (A_{ji} + N_e C_{ji}) + \sum_{k > j} N_e C_{jk} \right] = \\ = \sum_{i < j} N_i [R_{ij} + N_e C_{ij}] + \sum_{k > j} N_k [A_{kj} + N_e C_{kj}], \end{aligned} \quad (4)$$

N_e is the electron density, C the collision rate, and R_{ij} are the photo-excitation rates.

The collision rates are expressed in terms of the collision strengths $\Omega(i, j)$ in the form

$$C_{ij} = 8.63 \times 10^{-6} \Omega(i, j) \exp(-E_{ij}/KT_e) / \omega_i T_e^{1/2} \text{ (cm}^3 \text{ s}^{-1}\text{)} \quad \text{(for excitations),} \quad (5)$$

$$C_{kj} = C_{jk} \left(\frac{\omega_j}{\omega_i} \right) \exp(E_{jk}/KT_e) \text{ (cm}^3 \text{ s}^{-1}\text{)} \quad \text{(for de-excitations),} \quad (6)$$

where T_e is the electron temperature, K the Boltzmann constant, and E_{ij} is the excitation energy.

5. Integrated Line Fluxes

Integrated line fluxes has been computed using the solar model atmosphere of Elzner (1976). The emission per unit volume is given by the expression

$$E(j, i) = A_{ji} h \nu_{ij} N_j = \frac{1.59 \times 10^{-8}}{\lambda (\text{\AA})} A_{ji} \frac{N_j}{N_{\text{ion}}} \frac{N_{\text{ion}}}{N_{\text{el}}} \frac{N_{\text{el}}}{N_{\text{H}}} N_e \text{ (ergs cm}^{-3} \text{ s}^{-1}\text{)}, \quad (7)$$

where $N_{\text{H}} = 0.8N_e$ has been used. Integrated line flux (F) at Earth distance is given by

$$F = \frac{1}{2} \frac{\int E^*(j, i) 4\pi R_{\odot}^2 N_e dh}{4\pi (1 \text{ AU})^2} = \frac{1}{2} \left(\frac{R_{\odot}}{1 \text{ AU}} \right)^2 \int E^*(j, i) N_e dh \text{ (ergs cm}^{-2} \text{ s}^{-1}\text{)}, \quad (8)$$

where

$$E^*(j, i) = 1.59 \times 10^{-8} A_{ji} (N_j/N_{\text{ion}}) \left(\frac{N_{\text{ion}}}{N_{\text{el}}} \right) \left(\frac{N_{\text{el}}}{N_{\text{H}}} \right) \frac{1}{\lambda (\text{\AA})}.$$

R_{\odot} is the solar radius and 1 AU is one astronomical unit of distance. $N_{\text{ion}}/N_{\text{el}}$ has been taken from Jordan (1969). N_e and T_e as a function of height have been taken from Elzner's model. The chemical abundance $N_{\text{el}}/N_{\text{H}}$ for Mg and Si have been taken from Kato (1976). Factor $\frac{1}{2}$ in Equation (8) takes into account the fact that half the radiation thus produced leaves the Sun and the remaining half is emitted downward and absorbed in the photosphere (cf. Pottasch, 1964). Taking all these parameters into account, the absolute fluxes for various strong and weak lines emitted from 20 level scheme and received at Earth distance have been computed using Equation (8). Various significant line fluxes obtained from these computations have been given in Tables I and II for Mg VIII and Si X, respectively. In Tables I and II only those observed values are listed which correspond to the entire solar disc. We find that the calculated line fluxes in general are smaller than the corresponding observed values. The observed values are available for certain lines and in general are higher by a factor of two compared to the calculated ones.

TABLE I
 Calculated fluxes from the entire solar disk at Earth's distance.
 Mg VIII-ion; $n(\text{Mg})/n(\text{H}) = 3.16 \times 10^{-5}$

Transition	Wavelength Å	Flux (10^{-3} ergs cm^{-2} s^{-1})	
		Calculated	Observed
(19, 1)	74.86 ^b	0.48	1.5*
(20, 2)	75.03	0.75 } 0.10 }	2.2*
(19, 2)	75.04		
(16, 1)	82.60	0.12	
(16, 2)	82.82	0.25	
(10, 1)	311.81	1.05	
(9, 1)	313.74	1.92	
(10, 2)	315.02	5.40	
(9, 2)	317.03	1.35	
(8, 1)	335.23	0.95	
(8, 2)	338.95	1.27	
(6, 1)	430.47	1.74	3.09**
			(Blend with Mg VII)
(7, 2)	436.62	2.75	4.91**
			(Blend with Ne VI)
(6, 2)	436.73	0.30	
(5, 2)	783.60	0.10	
(4, 2)	794.20	0.08	
(2, 1)	3.03 μ	0.01 [†]	

^b Denotes blend.

* Observed values from Malinovsky and Heroux (1973).

** Observed values from Dupree *et al.* (1973).

[†] Observed line by Munch *et al.* (1967); Olsen *et al.* (1971).

6. Results and Discussion

Since the occupation of higher levels is essentially determined by the levels of the ground state, the variation of occupation of ground state levels is reflected in the variation of line emission. The relative ion abundance peaks at a particular temperature and, therefore, it is reasonable to assume that the line is emitted from a thin layer of effectively uniform electron density and temperature. In Figure 2 we have shown the relative population of ground state levels as a function of electron density for Mg VIII and Si X. We find that level population of the ground state levels vary with electron density. In Figures 3 and 4 we have shown various line intensity ratios for Mg VIII and Si X, respectively as a function of electron density. The temperature of $T_e = 8 \times 10^5$ K for Mg VIII and $T_e = 1.6 \times 10^6$ K for Si X are the typical values at which the relative ion abundance of the element has been reported to be maximum. In order to study the temperature dependence of line intensity ratios, we have also carried out computation at two different temperatures on either side of the temperature at which the relative ion abundance of element is maximum. We have shown in

TABLE II
 Calculated fluxes from the entire solar disk at Earth's distance.
 Si x-ion; $n(\text{Si})/n(\text{H}) = 5.01 \times 10^{-5}$

Transition	Wavelength Å	Flux (10^{-3} ergs cm^{-2} s^{-1})	
		Calculated	Observed
(19, 1)	50.52	2.09	
(20, 2)	50.69	0.78	
(19, 2)	50.70	0.42	
(16, 1)	54.79	0.30	
(16, 2)	55.01	0.62	
(10, 1)	253.81	1.31	2.5*
(9, 1)	256.58 ^b	3.86	14.0*
(10, 2)	258.39	6.61	13.5*
(9, 2)	261.27	3.18	6.8*
(8, 1)	272.00	3.15	5.5*
(8, 2)	277.27 ^b	2.31	4.7*
(6, 1)	347.43	5.61	
(7, 2)	356.07	1.98	
(6, 2)	356.10	0.77	
(5, 2)	653.00	0.07	
(4, 2)	638.00	0.14	
(2, 1)	1.43 μ	0.55 [†]	

^b Denotes blend, m denotes that line is masked.

* Observed values from Malinovsky and Heroux (1973).

† Observed line by Munch *et al.* (1967); Olsen *et al.* (1971).

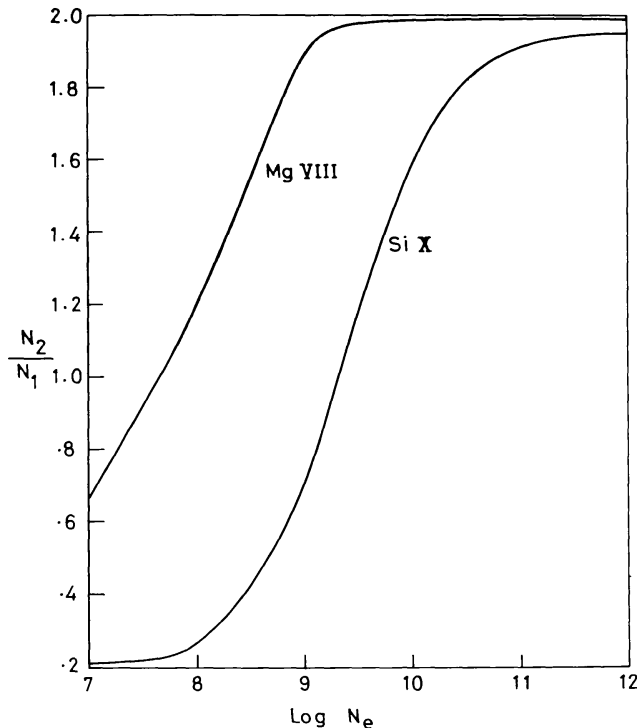


Fig. 2. Relative population of ground state levels (N_2/N_1) as a function of log of N_e .

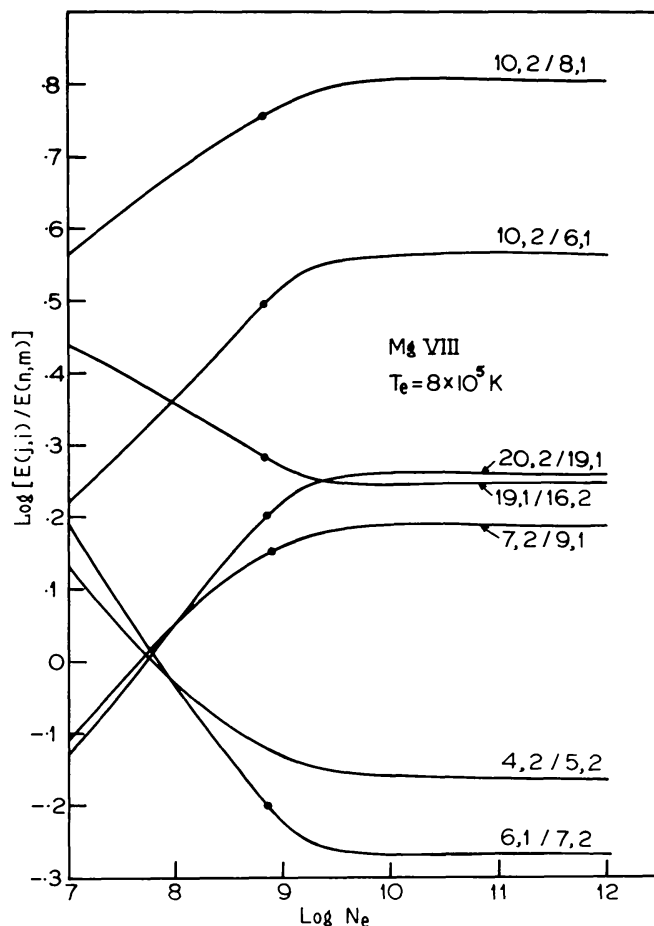


Fig. 3. Log of intensity ratios $E(j, i)/E(n, m)$ of Mg VIII lines as a function of log of N_e . Dots correspond to the calculated intensity ratios based on the model of Elzner (1976). T_e corresponds to the temperature for the maximum relative ion abundance of the element.

Table III the line intensity ratio for one pair of lines of Mg VIII at three different temperatures. Similar analysis has been made for other intensity ratios obtained. We find that the line intensity ratios shown in Figures 3 and 4 are insensitive of temperature variations.

TABLE III

Intensity ratios of 430.47 Å and 436.62 Å Mg VIII lines at three different temperatures, for $10^7 \leq N_e \leq 10^{12}$

Electron density (cm^{-3})	10^7	10^8	10^9	10^{10}	10^{11}	10^{12}
Log $E(6, 1)/E(7, 2)$ $T_e = 3 \times 10^5$ K	0.19	-0.02	-0.21	-0.24	-0.26	-0.28
Log $E(6, 1)/E(7, 2)$ $T_e = 8 \times 10^5$ K	0.19	-0.03	-0.22	-0.26	-0.26	-0.28
Log $E(6, 1)/E(7, 2)$ $T_e = 1.8 \times 10^5$ K	0.19	-0.02	-0.22	-0.26	-0.27	-0.29

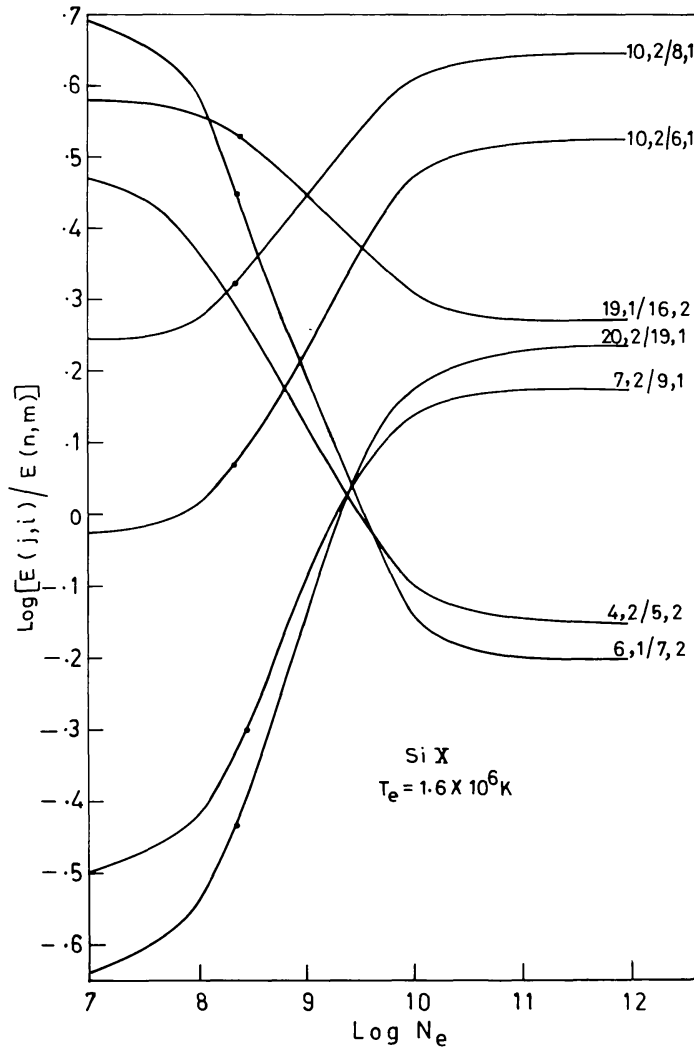


Fig. 4. Same as Figure 3 but for Si x lines.

In Figure 3 and Table III we see that the intensity ratio (6, 1)/(7, 2) of line at 430.47 \AA (transition $^2D_{3/2} - ^2P_{1/2}^o$) relative to the line at 436.62 \AA (transition $^2D_{5/2} - ^2P_{3/2}^o$) is found to be very sensitive to electron density variation for $N_e < 10^{10} \text{ cm}^{-3}$. For higher densities, the levels of the ground $^2P^o$ term are populated according to Boltzmann distribution. At lower densities, the radiative processes become important. Figure 2 further illustrates this point that the level populations of the ground state depend on the electron density ($N_e < 10^{10} \text{ cm}^{-3}$). Therefore, the line intensity ratios which are excited from the ground levels and emitted from different excited levels are sensitive to electron density, providing a direct method to determine N_e .

Dupree *et al.* (1973) have quoted the measured values of quiet Sun intensities for two lines of Mg VIII, namely 430.47 \AA and 436.62 \AA lines. The measured intensities of 430.47 \AA and 436.62 \AA are 22.7 and $36.1 \text{ ergs cm}^{-2} \text{ s}^{-1} \text{ sr}^{-1}$, respectively (Dupree *et al.*, 1973). Vernazza and Reeves (1978) have also reported the intensity of these lines. Vernazza and Mason (1978) have interpreted the measured line intensity ratios

(Vernazza and Reeves (1978) by arbitrary scaling of atomic data. Vernazza and Mason (1978) have increased the 430.47 Å line collision rate by 15% and reduced the 436.62 Å line collision rate by 15% to develop a best fit with the measurement for the active regions and the flare conditions. Unless the scaling up and scaling down of atomic parameters is justifiable in terms of physical changes taking place in the active regions and flare conditions, this seems quite artificial to match the measured data with the theoretical calculations. The spectral resolution of Vernazza and Reeves (1978) measurement is 1.6 Å. This could lead to incorrect interpretation of measured line intensity ratio of two lines because of blending of one line with another line in the vicinity arising from certain transitions in another ion. This happens to be the case for Mg VIII lines. For example the 430.47 Å line of Mg VIII may be blended with 431.3 Å line of Mg VII which belongs to the carbon sequence. Similarly, 436.62 Å line of Mg VIII may be blended with Ne VI line at 435.6 Å. In order to obtain the observed intensity ratio for the two Mg VIII lines, one must subtract the respective contributions of Mg VII and Ne VI line intensities from the actual observed values. To estimate these corrections we have proceeded as follows. Ne VI has two lines 562.80 Å and 435.65 Å whose transitions have the common lower level. Line at 562.80 Å is unblended. Using the oscillator strengths for these two transitions (Dankwort and Trefftz, 1978), we find that the expected intensity ratio of the 435.65 Å to that of 562.80 Å is 0.37. Observed intensity of the line 562.80 is $13 \text{ ergs cm}^{-2} \text{ s}^{-1} \text{ sr}^{-1}$ (Dupree *et al.*, 1973). Thus, the line 435.65 Å would have an intensity of $4.80 \text{ ergs cm}^{-2} \text{ s}^{-1} \text{ sr}^{-1}$. Mg VIII has two very closely spaced lines around 436 Å. After taking into account the contribution of Ne VI line, the combined observed intensity of Mg VIII lines around 436 Å would be $31.3 \text{ ergs cm}^{-2} \text{ s}^{-1} \text{ sr}^{-1}$. This amounts to a flux of $4.26 \text{ ergs cm}^{-2} \text{ s}^{-1}$ at Earth distance. According to our calculations the weaker component of this line pair has a flux one tenth of the total. Thus, the observed flux for the line at 436.62 should be $3.83 \text{ ergs cm}^{-2} \text{ s}^{-1}$. Assuming that for the two lines of Mg VIII (430.47 Å, 436.62 Å), the observed flux ratio is the same as the computed ratio, the expected observed flux in the line 430.47 Å should be $2.44 \text{ ergs cm}^{-2} \text{ s}^{-1}$. Therefore, we infer that the arbitrary scaling up or scaling down of the collision rates is not required to explain the observed line intensity ratio. There are other pairs of lines shown in Figure 3 which show similar density dependence and may prove to be useful for density determinations. The separation between X-ray lines is small, therefore, with greater spectral resolution, one can also use X-ray line pairs for density diagnostic. In Figures 3 and 4 we have shown by dots, the different intensity ratios obtained using integrated line fluxes from the model atmosphere of Elzner (1976).

We have shown in Figure 4, the variation of line intensity ratios of Si x lines with the electron density. Flower and Nussbaumer (1975b) have also calculated line ratios for three of the sets of lines shown in Figure 4. These are the line ratios (10, 2/6, 1), (10, 2/8, 2) and (6, 1/7, 2). Our results for these three ratios essentially agree with those of Flower and Nussbaumer. According to Dupree *et al.* line 347.43 of Si x may be blended with lines of Fe x, Fe XI, and Fe XII. Line 356.07 of Si x seems to blend

with Fe XIV line as indicated in Vernazza and Reeves' article. The spectral resolution is the same in Dupree *et al.* and Vernazza and Reeves papers. So blending is a serious problem in obtaining the observed intensity ratios of relevant lines. Thus we find that for ions namely Mg VIII and Si X the scaling up and scaling down of the atomic data have been used for obtaining a good fit between the measured and calculated line intensity ratios (Vernazza and Mason, 1978). However, we have shown that in case of Si X ion of the same isoelectronic sequence, such a modification of the atomic data is not needed for the required fit of the measured and calculated line intensity ratios. Further, we notice that the scaling up and scaling down of the atomic data by 15% at the same time may correspond to an error of 30% which is barely justifiable. Instead we believe that the blending of one line by other lines in the vicinity would affect the line intensity ratio. The measurement of line intensities with improved spectral resolution may provide the needed clue in this regard.

Finally, we have shown in Figure 5 the line emission per unit volume against height in the model atmosphere of Elzner (1976) for some of the intense lines of Mg VIII. This diagram indicates the contribution of the various atmospheric layers to the total

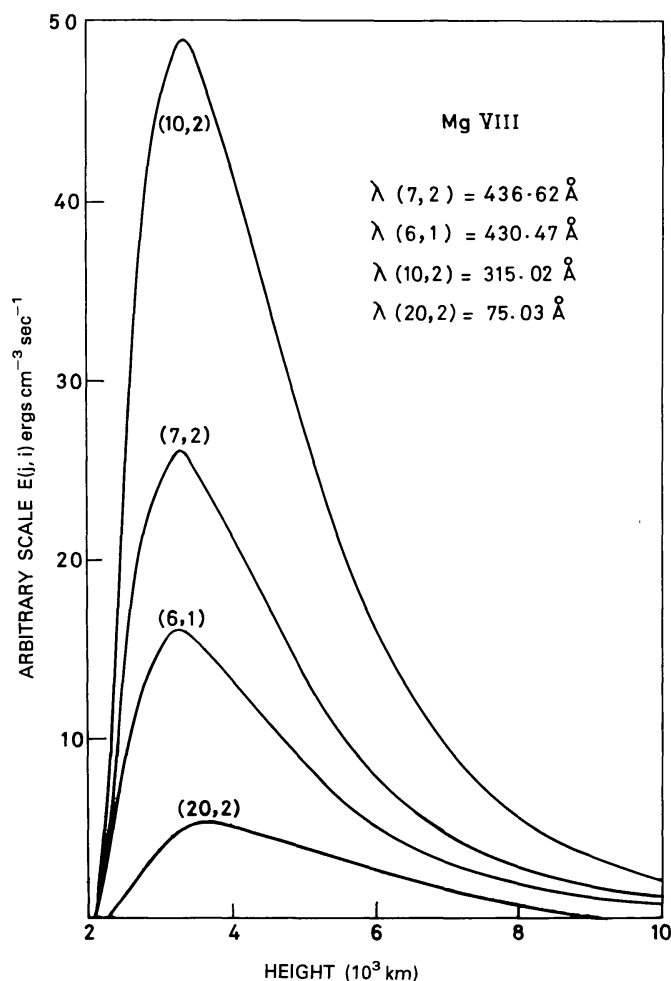


Fig. 5. Emission per unit volume (in units of $(N_{ei}/N_H) \times$ arbitrary scale factor) against height in the model atmosphere of Elzner (1976) for Mg VIII lines.

flux. We notice that the emission comes mainly from a narrow region having effectively uniform electron density and temperature. However, in case of Si x, corona also contributes to the total flux.

7. Conclusion

A number of line intensity ratios in Mg VIII and Si x line emission spectrum have been found to be density sensitive. Some of these ratios can be used as a density monitor of the emitting regions of the solar atmosphere. The integrated line fluxes calculated for a model solar atmosphere are useful in overcoming difficulties associated with line identification and blending of two close lines. The scaling up and scaling down of atomic data for developing a good fit between calculated and observed line intensity ratios seems unnecessary. The proposition that the blending of two close lines may affect the line intensity ratios needs serious consideration and calls for measurements with improved spectral resolution.

Acknowledgements

We are thankful to Prof. R. N. Singh, Institute of Technology, Banaras Hindu University, Varanasi for useful discussions and valuable suggestions. One of us (B. N. Dwivedi) is thankful to Dr M. K. V. Bappu, Director, Indian Institute of Astrophysics, Bangalore for encouragement. Thanks are also due to an unknown referee for valuable suggestions.

References

- Allen, C. W.: 1973, *Astrophysical Quantities*, Athlone Press, London.
- Bely, O. and Faucher, P.: 1970, *Astron. Astrophys.* **6**, 88.
- Dankwort, W. and Treffitz, E.: 1976, *Astron. Astrophys.* **47**, 365.
- Dankwort, W. and Treffitz, E.: 1977, *J. Phys. B, Atom. Molec. Phys.* **10**, 2541.
- Dankwort, W. and Treffitz, E.: 1978, *Astron. Astrophys.* **65**, 93.
- De Boer, K. S., Olthof, H., and Pottasch, S. R.: 1972, *Astron. Astrophys.* **16**, 417.
- Dufton, P. L., Berrington, K. A., Burke, P. G., and Kingston, A. E.: 1978, *Astron. Astrophys.* **62**, 111.
- Dupree, A. K., Huber, M. C. E., Noyes, R. W., Parkinson, W. H., Reeves, E. M., and Withbroe, G. L.: 1973, *Astrophys. J.* **182**, 321.
- Dwivedi, B. N.: 1979, Doctoral Thesis, Banaras Hindu University, Varanasi, India.
- Elwert, G. and Raju, P. K.: 1975, *Astrophys. Space Sci.* **38**, 369.
- Elzner, L. R.: 1976, *Astron. Astrophys.* **47**, 9.
- Flower, D. R. and Nussbaumer, H.: 1975a, *Astron. Astrophys.* **45**, 145.
- Flower, D. R. and Nussbaumer, H.: 1975b, *Astron. Astrophys.* **45**, 349.
- Gabriel, A. H. and Jordan, C.: 1972, in E. McDaniel and M. C. McDowell, *Case studies in Atomic Collision Physics*, Vol. II, North-Holland Publ. Co., p. 210.
- Jordan, C.: 1969, *Monthly Notices Roy. Astron. Soc.* **142**, 501.
- Jordan, C.: 1971, *Highlights of Astronomy* **2**, 519.
- Kato, T.: 1976, *Astrophys. J. Suppl.* **30**, 397.
- Kelly, R. L. and Palumbo, L. J.: 1973, 'Atomic and Ionic Emission Lines below 2000 Å', NRL Report 7599.

- Labs, D. and Neckel, H.: 1968, *Z. Astrophys.* **69**, 1.
- Loulergue, M. and Nussbaumer, H.: 1976, *Astron. Astrophys.* **51**, 163.
- Malinovsky, M. and Heroux, L.: 1973, *Astrophys. J.* **181**, 1009.
- Munch, G., Neugebauer, G., and McCammon, D.: 1967, *Astrophys. J.* **149**, 681.
- Munro, R. H., Dupree, A. K., and Withbroe, G. L.: 1971, *Solar Phys.* **19**, 347.
- Olsen, K. H., Anderson, C. R., and Stewart, J. N.: 1971, *Solar Phys.* **21**, 360.
- Pottasch, S. R.: 1964, *Space Sci. Rev.* **3**, 816.
- Raju, P. K.: 1978, *Bull. Astron. Soc. India* **6**, 45.
- Raju, P. K. and Dwivedi, B. N.: 1978, *Solar Phys.* **60**, 269.
- Raju, P. K. and Dwivedi, B. N.: 1979, *Pramana* **13**, 319.
- Shamey, L. J.: 1971, *J. Opt. Soc. Am.* **61**, 942.
- Vernazza, J. E. and Mason, H. E.: 1978, *Astrophys. J.* **226**, 720.
- Vernazza, J. E. and Reeves, E. M.: 1978, *Astrophys. J. Suppl.* **37**, 485.
- Wiese, W. L., Smith, M. W., and Miles, B. M.: 1969, *Atomic Transition Probabilities*, Vol. 2, Sodium through Calcium, US Dept. of Commerce, Nat. Bur. Standards.